LEAK DETECTION AND LOCATION IN A REAL WATER DISTRIBUTION NETWORK USING A MODEL-BASED TECHNIQUE

Bruno Ferreira[1], Nelson Carriço[2] and Dídia Covas[3]

[1,2]INCITE, Barreiro School of Technology, Polytechnic Institute of Setúbal, Setúbal, Portugal
[3]CERIS, Instituto Superior Técnico, Universidade de Lisboa, Lisbon, Portugal

[1] bruno.s.ferreira@estbarreiro.ips.pt, [2] nelson.carrico@estbarreiro.ips.pt,
[3] didia.covas@tecnico.ulisboa.pt

Abstract

This paper presents a practical application of a model-based approach for leak detection and location in a real water distribution network. The methodology is divided into three main steps: 1) identification of the DMA with the highest leakage volume; 2) hydraulic model update and 3) leak location by inverse analysis. The water distribution network is monitored through 14 flowrate and pressure sensors and data were available for 1.5 years. The methodology is applied 15 times, specifically to five weekdays in three different periods with high seasonal variation (summer, spring and winter). Regardless of the analysed period, obtained results point to the presence of a leak with ca. 4 m³/h in a specific area of the network. This approximate location is a starting point for the application of more precise leak location techniques using acoustic equipment.

Keywords
Leakage identification, Leakage location, Hydraulic simulation, Minimum night flow, Optimization.

1 INTRODUCTION

The occurrence of pipe bursts represent an important source of water losses in water distribution networks (WDN), depending on their frequency and size. Users usually report events to utilities when surface flooding or service disruption occurs. The problem lies in events that do not cause water to come up to the surface, nor cause service disruption. These events can continue unreported for a long time, potentially leading to the loss of large volumes of water and the consumption of energy and water disinfectants, whilst also posing a health risk to the population due to risks of bacteria and pollutant contamination [1].

The first step towards an efficient leakage management is the accurate assessment for the water volume that is lost. To this end, WDN are usually divided in smaller district metered areas (DMA) in which the flowrates are continuously measured in the area's inlets and outlets and the consumed water volume is periodically measured in consumers. Leakage volumes in DMA are usually assessed through the the minimum night flow (MNF) regime [2,3]. During the MNF, consumption from users is usually minimum and the dominant consumption is due to leakage. Such MNF analysis can reduce the search area from the whole WDN to a particular DMA. Nonetheless, additional burst and leak location techniques are necessary to find the approximate location inside the DMA and the exact location at the street level.

Leak location techniques generally involve the use of acoustic equipment (e.g., listening rods and leak correlators) or of non-acoustic methods (e.g. gas tracer injection, ground-penetrating radar, or infrared photography) [4]. Although accurate, these equipment-based inspection techniques are time-consuming and labor-intensive processes, even in relatively small DMA [5]. Thus, a software-based approach is should be used before to reduce the search area to a particular zone in the DMA (e.g., at the street level).

Distinct software-based techniques have been developed in last decades for leak detection and location in WDN. These techniques can be roughly divided in model-based and data-driven methods. Data-driven methods [6–8] use monitoring data that, combined with tools such as data mining or artificial intelligence algorithms, allow the identification of possible leak location zones [9]. Although these methods do not require a deep knowledge regarding the WDN hydraulic characteristics (e.g., pipe characteristics or individual demands), extensive historical data records of monitoring data and precise information on past pipe burst events are necessary. In many water utilities, service work orders are collected by operational technicians who register imprecise and incomplete data [10].

Model-based methods use a hydraulic simulation models and detect and locate leaks based on the comparison of numerical results with measurements from pressure sensors and flowrate meters. Examples of these methods are the inverse analysis [11–13], the network sensitivities' computation and analysis [14,15], the error-domain model falsification [16,17], or based on a classification problem [18,19]. Although promising results have been obtained using these methods (see [13,20]), their application usually requires a robust and well calibrated hydraulic model and a high number of pressure sensors with long time-records. In addition, obtained results are highly sensitive to the uncertainty of model parameters (e.g., water consumption, valve states, and pipe characteristics).

This paper presents the practical application of a model-based approach for leak detection and location in a real WDN located in Porto Metropolitan Area, in Portugal. The network has a total length of 37 km and serves 996 consumers, being divided in seven DMA. The water utility has identified the existence of a leak by analysing the minimum night flow. The leak location is known to be somewhere in an area along the embankment of a river, whose flow affects the noise captured by the acoustic equipment. In this context, the water utility challenged the authors to apply a model-based technique and find the leak location. This approximate location will be the starting point for the application of more precise leak location techniques using acoustic equipment. Data were collected in 14 sensors (seven pressure transducers and seven flowmeters) during the period between 1st of June 2020 and 26th of December 2021. The number and location of pressure and flowrate sensors were established by the water utility to monitor DMA (inlets and outlets) both in terms of water consumption and pressure requirements. The model-based methodology is applied to 15 different days divided into three periods (with different data availability). Genetic Algorithms [21] are used as the optimization method. Obtained results are discussed and the most relevant conclusions are drawn, focusing on the difficulties of implementing model-based techniques to leakage location in real-life contexts.

2 METHODS

The used model-based methodology is divided in three main steps: 1) identification of the DMA with the highest leakage volume; 2) hydraulic simulation model update and 3) leak location by inverse analysis. The first step is aims at identifying the DMA with highest leakage volumes based on the analysis of the MNF and at estimating the burst magnitude. The hydraulic simulation model should be updated with the water consumption and valve settings corresponding to the collected data period. Finally, the leak/burst is located by formulating and solving the inverse problem. The objective is to determine the values of the unknown parameters (leak location and size) in the hydraulic model that minimizes the difference between numerical results and real measurements. These steps are further explained in the following sections.

2.1 Identification of the DMA with the highest leakage volume

A simple yet effective method is proposed herein to identify the DMA with the highest leakage volume, as well as to roughly estimate the respective size. Two metrics may be calculated for this purpose for each DMA by considering a complete day of measurements. The first metric (M1)

quantifies the average water consumption during the MNF per service connection (SC) [m³/(h.SC)] in each DMA. During the MNF, the user water consumption is minimum, the network pressure is high and, thus, the leak volume has the highest contribution to the flowrate. The second metric (M2) quantifies the average daily consumption per service connection [L/(day.SC)]. The water losses can be assessed in each DMA by comparing the metrics M1 and M2 values for DMA with similar characteristics (e.g., similar size or topology) and by assessing if any DMA presents outlier values of these metrics. The first metric aims to assess if unexpected consumption is occurring during the night whilst the second metric aims to assess if unexpected consumption is occurring throughout the day. The occurrence of outlier metric values for a DMA indicate that every service connection of that DMA is presenting (on average) an abnormally high water consumption during either the night (for the first metric) or through the day (for the second metric).

Once the DMA with a high leakage level has been identified, the leak volume can be estimated. To this end, the average of metric M1 values (without the outlier values) should be calculated for DMA with similar characteristics. This value (in m³/[h.SC]) should be multiplied by the number of SC in the DMA with leakage. This allows estimating the MNF (in m³/h) in a no-leakage scenario. Finally, the leak size (in m³/h) can be estimated by subtracting the MNF in the no-leakage scenario from the real MNF.

This analysis can be carried out for distinct periods (e.g., summer or winter, weekdays or weekends) to validate the identified DMA with high leakage levels.

2.2   Hydraulic simulation model update scheme

The application of the leak location technique described in 2.3 requires the use of a hydraulic model of the WDN. To guarantee reliable results, it is essential to minimize the uncertainty in model parameters (which arise predominantly from water consumption [17]). This can be achieved by updating the hydraulic simulation model with the actual water consumption values that occurred (minus the effect of the leak) during the period for which the leak location analysis will be performed. If telemetry at the user level is available, the hydraulic simulation model can be updated with the individual consumption of each user (e.g., through an individual daily measurement). In most cases, the individual consumption of each user is unknown and only the total consumption of each DMA is known. In these situations, a consumption pattern for each DMA can be created (and is equal to the DMA consumption); the base demand of each node (of each DMA) represents the proportion of the consumption of that specific node concerning the overall DMA. This proportion can be obtained, for instance, based on the billing records (i.e., the amount of billed water).

In addition to water consumption, boundary conditions must be properly updated. These include settings for valves, pumps, and tanks. For this purpose, specific time step controls can be developed if measurements are available (e.g., a rule can be created for the setting of a PRV based on the outlet pressure measurements of the PRV).

2.3   Leak location

The leak location can be carried out by solving the inverse problem, that is, by finding the values of the unknown parameters (leak size and location) in the hydraulic model, that minimize the differences between numerical results and real measurements [11–13].

Consider the N vector containing the indexes of all potential leak locations (e.g., all node) in the DMA identified in 2.1. A single-objective optimization problem is formulated and two decision variables are considered, namely, the leakage location (defined as a discrete variable that may assume any value in N) and the leakage size (i.e., the value of the emitter coefficient C, defined as a continuous variable). Two types of constraints are considered, namely, a set of implicit type constraints considering hydraulics systems (which are guaranteed by the hydraulic solver) and

an additional constrain which bound the algorithm solution search space by avoiding solutions that may cause negative pressures in the system. The optimization problem can be formulated as follows:

$$Search\ for\ X = [L_i, C_i];\ L_i\ \in N$$
$$Minimize\ F(x) \tag{1}$$
$$Subject\ to\ P_i > 0$$

where L_i and C_i are the node index and emitter coefficient value for leakage in location i, N is the vector containing the indexes of all nodes in the DMA, and P_i is the pressure at location i (for the leak scenario).

Finally, the objective function $F(X)$ is defined as the weighted sum of squared differences between real and simulated values for both pressure and flowrate at the measurement nodes (assuming a leak in location L_i and size C_i) as follows:

$$F(X) = \sum_{k=1}^{T} \left[\sum_{s=1}^{N_p} \frac{(\frac{P_{sensor\ s}^{real}(k) - P_{sensor\ s}^{sim}(k)}{P_{pnt}})^2}{N_p} + \sum_{q=1}^{N_q} \frac{(\frac{Q_{sensor\ q}^{real}(k) - Q_{sensor\ q}^{sim}(k)}{Q_{pnt}})^2}{N_q} \right] \tag{2}$$

where N_p and N_q are the number of pressure and flowrate sensors, respectively; $P_{sensor\ s}^{real}(k)$ and $P_{sensor\ s}^{sim}(k)$ are, respectively, the real and simulated (with the leak in location L_i and size C_i) pressure values in sensor s with respect to time k; $Q_{sensor\ q}^{real}(k)$ and $Q_{sensor\ q}^{sim}$ are the real and simulated flowrate values in sensor q with respect to time k, respectively, and T is the total number of time steps considered in the analysis.

P_{pnt} is the average pressure measurement error (m) and is based on the average observed pressure values at sensor nodes and the pressure sensor reading percentage error as indicated by the manufacturer. Similarly, Q_{pnt} is the average flowrate measurement error (m³/h) as is based on the average global system demand and the flow reading percentage error.

3   APPLICATION: RESULTS AND DISCUSSION

3.1   Case study description

The case study is a WDN located in Porto Metropolitan Area, Portugal, with an overall network extension of around 37 km. The WDN is supplied by a single water tank and is divided into seven DMA. Pressure and flowrate measurements were collected through 14 sensors, installed in the inlets and outlets of the DMA, during the period between 1st June 2020 and 26th December 2021 with a 15-minute time step. The WDN is located in a hill, resulting in significant elevation differences between the water source (at 162 m) and the lowest point supply location (at 12 m). As such, pressure-reducing valves (PRV) are installed at different locations in the WDN to reduce excessive pressures. The hydraulic simulation model was developed in EPANET and includes one storage tank, 1,058 node junctions, 344 valves, and 728 pipes. Figure 1 presents a schematic representation of the WDN with the location of measuring points (MP) and the PRV in relation to the DMA inlet and outlets. The number of service connections of each DMA is also presented.
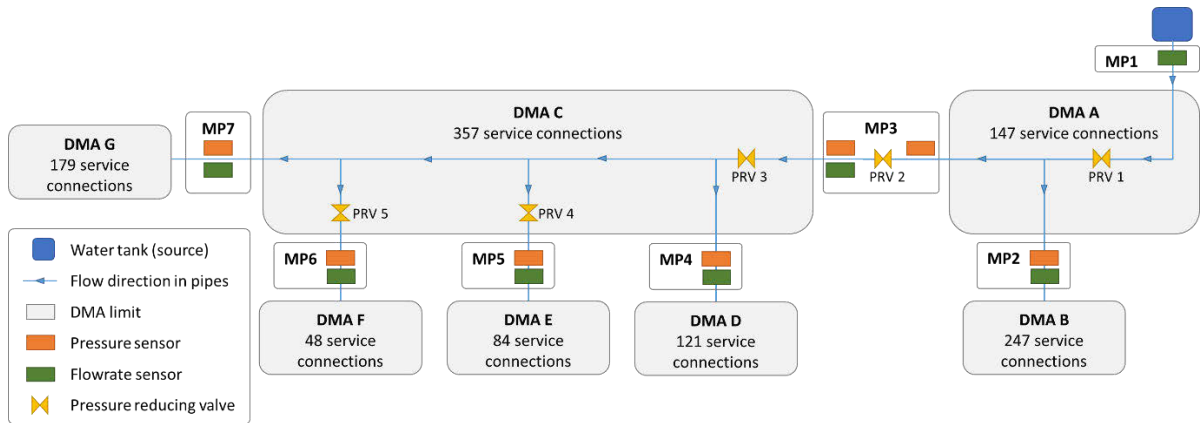
Figure 1. WDN scheme with the location of MP and PRV concerning the DMA inlet and outlets.

Figure 2 depicts the data availability for each of the sensors between 1st June 2020 and 26th December 2021. Although 14 sensors are installed in the network, there is not a single period where data from all the sensors is simultaneously available. The missing data are due to the fact that some sensors had not yet been installed (e.g., MP6 was only installed in September 2021) and due to sensor malfunction (in the remaining sensors with missing data). Based on the data availability, three distinct periods (of five weekdays) are selected for analysis: one week in august 2020 (period P1), one week in March 2021 (P2) and one week in December 2021 (P3).
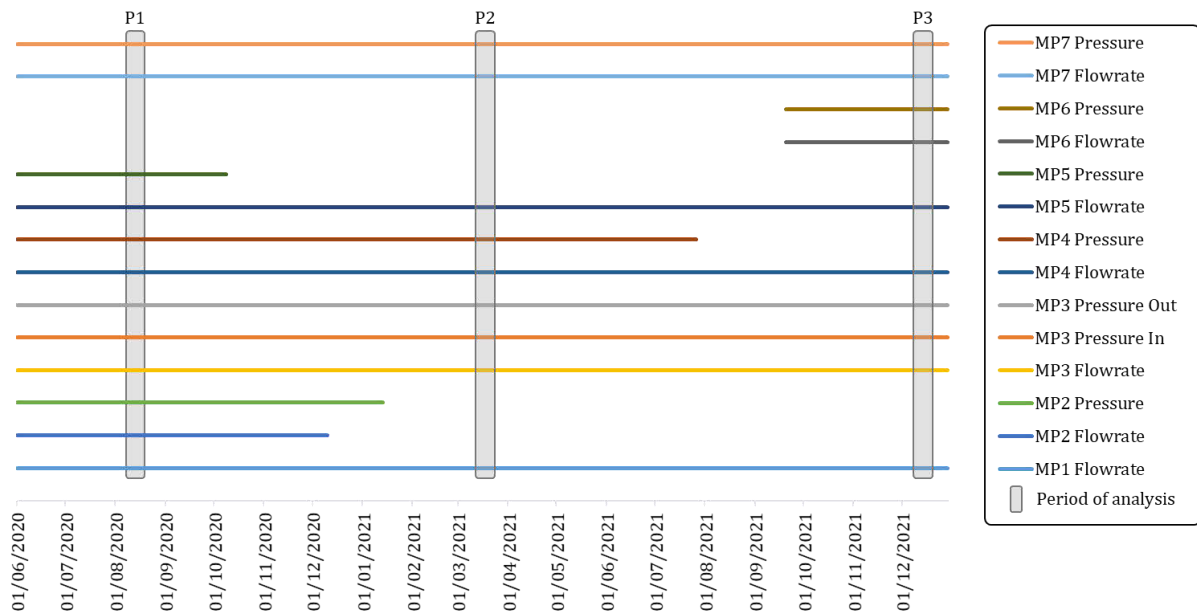

Figure 2. Data availability for the 14 sensors in the period from June 2020 to December 2021 (in horizontal bars) and selected periods for analysis (in vertical bars).

3.2 Identification of the DMA with the highest leakage volume

Leak detection is carried out based on the calculation of metrics M1 and M2 (as explained in 2.1) for each DMA. The metrics are calculated for every weekday of the three periods of analysis and the average metric values are computed in each of the three periods. This calculation requires the consumption values (in each time step) for each DMA to be known. This consumption is directly linked to the inlet flowrate measurements in *downstream* DMA (i.e., DMA B, D, E, F and G). However, in *intermediate* DMA (such as DMA A and C), this consumption is obtained by a water balance between inlets and outlets. For instance, the consumption of DMA C is obtained by a water

balance between the inlet (MP3) and the four outlets (MP4 to MP7). A similar process is applied to DMA A between the inlet (MP1) and the two outlets (MP2 and MP3).

Although the water balance is easily calculated, not all inlet/outlet values were available. This compromises the balance calculation of cascade DMA, since all the unaccounted demand for DMA with missing data is assumed as leakage. In these situations, an estimation of DMA consumption (in each time step) is carried out based on the average consumption per service connection in the remaining DMA.

Table 1 presents the average metric results (for the five weekdays) for each DMA in each period. The highest value of each column is highlighted in bold. DMA A presents no value for the first metric (in either period). The consumption of this area is calculated based on a water balance using data from sensors with different characteristics and measurement errors. Also, overestimation of water consumption for certain DMA might occur. As such, negative values for water consumption in this area are obtained (especially during the night period). In these time steps, the value of zero consumption is assumed, hence the value for the first metric. By assessing the first metric value, it is possible to conclude that leaks are present in several DMA. Nonetheless, DMA C is likely to have a major leak. Note that it is unlikely that, on average, each service connection (of the 357) in DMA C consumes more than double the amount of any service connection of the remaining DMA during MNF, regardless of the period of analysis. This is confirmed by the results of the metric M2, as it is unlikely that the average daily consumption of service connection in DMA C is more than double than in the remaining DMA. A more plausible explanation for the metric values in DMA C might be the existence of a major unknown leak/burst, which results in additional water consumption, both during the night and throughout the day.

Table 1. Average M1 and M2 values for each DMA during each period

DMA	SC	Week in August 2020 (P1)		Week in March 2021 (P2)		Week in December 2021(P3)	
		M1 [m³/(h.SC)]	M2 [L/(day.SC)]	M1 [m³/(h.SC)]	M2 [L/(day.SC)]	M1 [m³/(h.SC)]	M2 [L/(day.SC)]
DMA A	147	0	425	0	220	0	308
DMA B	247	0.0016	273	0.0031	300	0.0045	291
DMA C	357	**0.0157**	**610**	**0.0148**	**595**	**0.0177**	**646**
DMA D	121	0.0006	286	0.0003	232	0.0019	233
DMA E	84	0.0074	413	0.005	353	0.0035	271
DMA F	48	0.0035	334	0.0031	300	0.0068	334
DMA G	179	0.0032	366	0.0034	316	0.005	326

The estimation of leak/burst size in DMA C is carried out as described in 2.1. The leak size is estimated for each day of the three period as follows: 1) the average M1 values for DMAs (with the exception of DMA A and C) is calculated; 2) this value is multiplied by 357 (the number of service connections in DMA C) and a new MNF (without leakage) for DMA C is obtained; 3) the leak size is estimated by subtracting the new MNF (without leakage) from the real MNF.

Table 2 presents the average leak size (for the 5 weekdays) for each DMA in each period. Based on these results, the leak is estimated on 4 m³/h. The two exceptions (in period P2) can be associated with the overestimation of consumption values.

Table 1. Size of leakage in DMA C in distinct periods

	Leakage size [m³/h]				
	Monday	Tuesday	Wednesday	Thursday	Friday
Week in August 2020 (P1)	4.64	4.51	4.54	4.26	4.33
Week in March 2021 (P2)	3.98	4.88	3.08	4.79	4.36
Week in December 2021(P3)	4.73	4.68	4.80	4.69	4.94

3.3 Hydraulic simulation model update

A total of 15 days (divided in 3 periods) are considered for the leak location analysis. As such, a total of 15 hydraulic simulation models (one for each day) are developed. In each model, two major update processes are carried out, namely, the water consumption of DMA and the settings of PRV.

The water consumption of each DMA is updated through a consumption pattern. Note that the base demand of each node (in each DMA) represents the proportion of the consumption of that specific node in relation to the overall DMA. Furthermore, the consumption of DMA C (where the leak is located) should be updated without the leakage effect. This is done by subtracting the leak size (as previously calculated) from the DMA C consumption in each time step. Figure 3 depicts the consumption pattern for each DMA on Monday, 13th December 2021, including the pattern for DMA C with (in dashed red line) and without (in solid red line) the major leak effect.
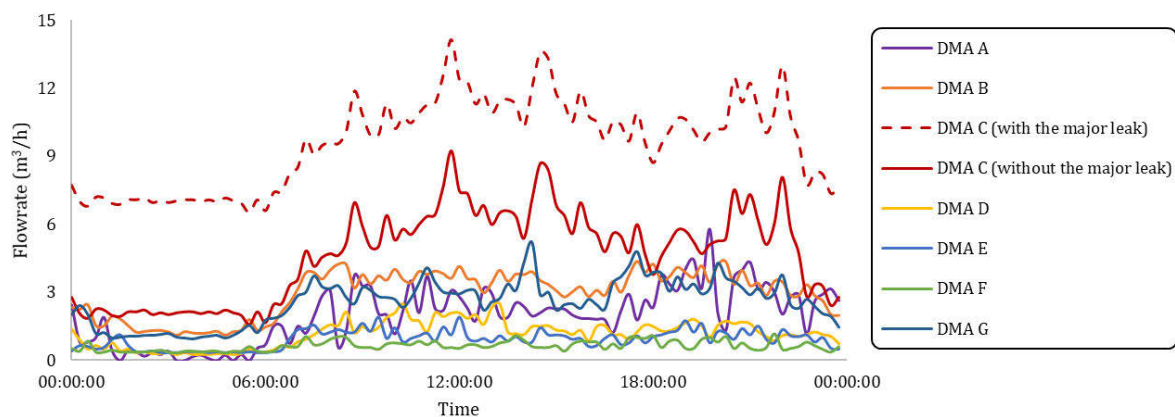

Figure 3. Consumption pattern for each DMA. The pattern for DMA C is depicted both with leakage (in dashed red line) and without leakage (in solid red line).

The second update process focuses on boundary conditions through controls of PRV settings. This is essential as PRV, although having a fixed service pressure value, often fluctuate around that value. Furthermore, time-controlled actions are often associated with such devices (e.g., for reduction of pressure during night hours) which must be accurately translated into the hydraulic simulation model. In this study, controls are created for PRVs 2, 4, and 5 based on the available measurements of PRV outlet pressure. Figure 4 exemplifies the update process of PRV 2, and its effect on MP7 (which is located further downstream). The default setting for PRV 2 is 35 m, as can be observed by the orange line. The value of 35 m may be adequate for the day period, as observed by the proximity of the orange line to the dark blue line. However, it is not adequate for the night period as these lines differ by approximately 10 m. Furthermore, the setup of PRV 2 directly influences the MP7; by considering a fixed set point of 35 m in PRV 2, an almost static pressure value of 110 m is observed in MP7 (in red line). By assigning the measured PRV 2 outlet pressure values (in dark blue line) to controls in the hydraulic simulation model, it is possible to obtain similar valve settings (as shown by the overlap of dark blue and dashed green lines). As a result, simulated and real measurements in MP7 (in dashed grey and green lines) vary just slightly; simulated pressures are in fact higher as a lower overall water consumption (since the leakage is

not modelled) is used. Lastly, real and simulated measurements in the inlet of PRV 2 differ greatly. Although modelling error might be present, the real pressure measurements values (around 80 m) are above the maximum possible value of 68 m (considering that the reservoir is located at 162 m of elevation, and the MP3 is located at 94 m). This indicates that a problem might exist with this sensor (either lacking calibration or within the measurement system itself) which, effectively, invalidates its usability.
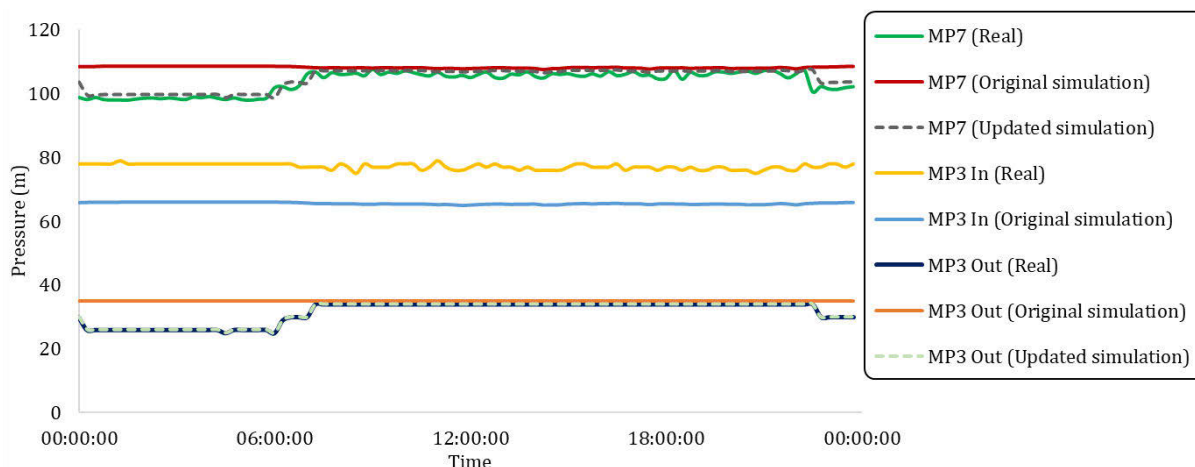

Figure 4. Effect of updating PRV 2 (with values MP3 Out) in the MP7

Although two additional PRV can be found in the network (PRV 1 and 3), they are not easily calibrated through the assignment of controls as no pressure sensor is placed downstream of those valves. As such, the fixed setting is used as provided by the water utility.

3.4 Leak location

Leak location is carried out as described in 2.3 for the night period in each day of each period (with a total number of 15 optimization runs). A specific hydraulic simulation model was prepared for each day (as described in 3.3). Hydraulic simulations are carried out in EPANET [22] by using the Water Network Tool for Resilience (WNTR) Python package [23]. The inverse problem is solved using Genetic Algorithms [21] with Pymoo Python package [24]. In problem formulation, all nodes of DMA C are considered as potential leak locations.

Three pressure sensors (MP2, MP4, and MP7) and two flowmeters (MP1 and MP3) are considered in the analysis for period P1. Due to data availability, two pressure sensors (MP4 and MP7) and two flowmeters (MP1 and MP3) are considered for the analysis in period P2. For period P3, a single pressure sensor (MP7) and two flowmeters (MP1 and MP3) are used. Many of the optimization problems lead to similar locations and, thus, from the total of 15 problems, only 3 distinct locations were obtained. Such locations are depicted in Figure 5 in blue circular markers and are grouped in a specific zone in DMA C (more specifically near the outlet to DMA G).
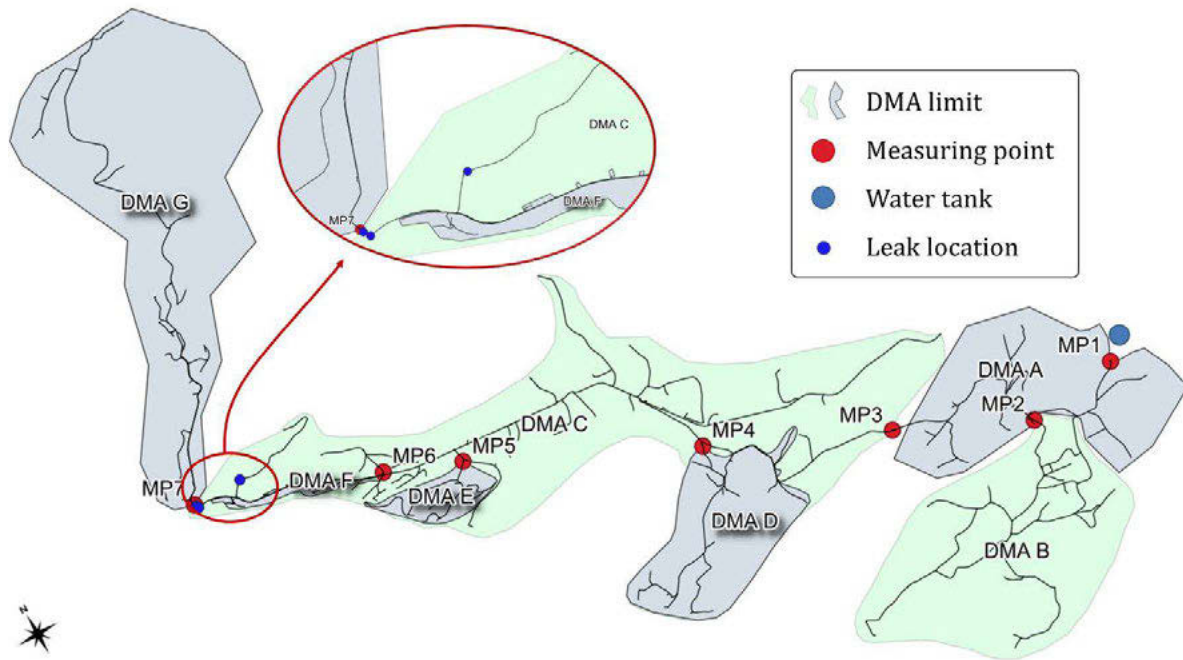
Figure 5. Obtained leak locations

Figure 6 depicts the simulated (after optimization) and real measurements for Monday, 13th December 2021. Although the optimization is carried out only for the night period, the simulated and real measurements are presented for the complete day. These results show that, after the optimization, real and simulated flowrate measurements (in MP1 and MP3) overlap almost perfectly. Pressure measurements (in MP4 and MP7) present small differences, most notably in MP7 during the night period. Such differences may be associated with additional head loss effects that are not considered in the analysis, for instance, unknown valve status, which induce local head losses.
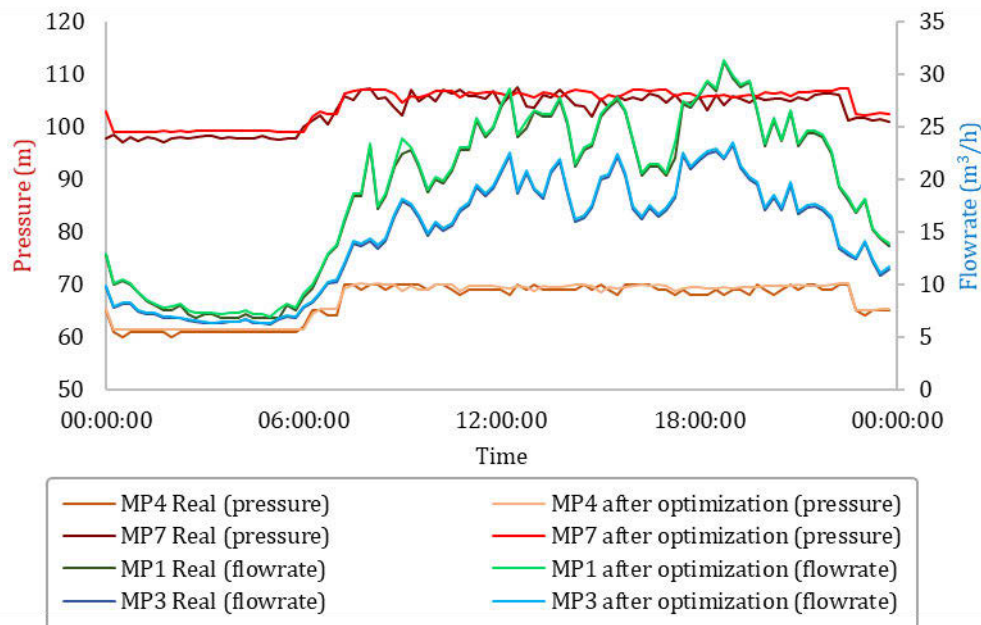

Figure 6. Comparison between simulated and real measurements after leakage location

By assessing the results of the three period, and based on the available sensors and data, it is possible to conclude that the leak may be located at downstream the DMA C. Note that the number

and location of pressure and flowrate sensors were established in order to monitor DMAs both in terms of water consumption and pressure requirements and not for leak location. Although such sensors can be used for leak location (as shown), their location is not optimized for that objective. This is a reality in many Portuguese water utilities, as investment in sensors is carried out mainly to monitor water consumption and inlet pressure of DMA. Ideally (and in addition to the already installed sensors), an optimal number of pressure sensors should be established, for instance, based on the analysis of the hypervolume indicator [25], and whose location is optimally defined to carry out leak detection and location [26].

4 CONCLUSIONS

This paper presents the practical application of model-based methodology for leak detection and location in a real WDN. The methodology is based on three main steps, namely: 1) identification of the DMA with the highest leakage volume; 2) hydraulic simulation model update (specifically water consumption and valve settings) and 3) leak location (by formulating and solving an inverse problem).

The WDN is monitored through 14 (flowmeter and pressure) sensors installed in the inlet and outlets of the seven DMA. Data are available over the period between the 1st of June 2020 and the 26th of December 2021. The methodology is applied 15 times, specifically to five weekdays in three periods (August 2020, March 2021, and December 2021). Results from the first step indicate that, regardless of the period being assessed, a leak with 4 m^3/h does exist in DMA C. In the second step, 15 hydraulic simulation models are developed by updating the real water consumptions (occurring during that period) and by creating valve controls (based on the measured PRV outlet pressure). Finally, 15 leakage locations are obtained in the third step by solving 15 optimization problems. Obtained leak locations point to a specific zone in the DMA C and should be treated as the starting point for the application of more precise leak location techniques in situ (e.g., acoustic equipment).

This study also demonstrates the difficulties of implementing model-based techniques for leak location in real-life contexts. Although large capital sums are already invested in network monitoring of water consumption and service pressure by water utilities, the installed sensors are often insufficient and non-optimally located. This is a reality in many Portuguese water utilities, which require further investment in network monitoring so that automatic model-based techniques for leak location can become a common practice in Portuguese water utilities.

5 ACKNOWLEDGMENT

6 REFERENCES

[1] Fontanazza, C.M., Notaro, V., Puleo, V., Nicolosi, P., and Freni, G. (2015). Contaminant intrusion through leaks in water distribution system: Experimental analysis. Procedia Engineering 119, 426–433. doi:10.1016/j.proeng.2015.08.904.

[2] Farah, E., and Shahrour, I. (2017). Leakage Detection Using Smart Water System: Combination of Water Balance and Automated Minimum Night Flow. Water Resources Management 31, 4821–4833. doi:10.1007/s11269-017-1780-9.

[3] Covas, D.I.C., Cláudia Jacob, A., and Ramos, H.M. (2008). Water losses' assessment in an urban water network. Water Practice and Technology 3, 1–9. doi:10.2166/wpt.2008.061.

[4] Li, R., Huang, H., Xin, K., and Tao, T. (2015). A review of methods for burst/leakage detection and location in water distribution systems. Water Science and Technology: Water Supply 15, 429–441. doi:10.2166/ws.2014.131.

[5] Moors, J., Scholten, L., van der Hoek, J.P., and den Besten, J. (2018). Automated leak localization performance without detailed demand distribution data. Urban Water Journal 15, 116–123. doi:10.1080/1573062X.2017.1414272.

[6] Loureiro, D., Amado, C., Martins, A., Vitorino, D., Mamade, A., and Coelho, S.T. (2016). Water distribution systems flow monitoring and anomalous event detection: A practical approach. Urban Water Journal 13, 242–252. doi:10.1080/1573062X.2014.988733.

[7] Gomes, S.C., Vinga, S., and Henriques, R. (2021). Spatiotemporal Correlation Feature Spaces to Support Anomaly Detection in Water Distribution Networks. Water 13, 2551. doi:10.3390/w13182551.

[8] Romano, M., Kapelan, Z., and Savić, D.A. (2014). Automated Detection of Pipe Bursts and Other Events in Water Distribution Systems. Journal of Water Resources Planning and Management 140, 457–467. doi:10.1061/(ASCE)WR.1943-5452.0000339.

[9] Wu, Y., and Liu, S. (2017). A review of data-driven approaches for burst detection in water distribution systems. Urban Water Journal 14, 972–983. doi:10.1080/1573062X.2017.1279191.

[10] Carriço, N., Ferreira, B., Barreira, R., Antunes, A., Grueau, C., Mendes, A., Covas, D., Monteiro, L., Santos, J., and Brito, I.S. (2020). Data integration for infrastructure asset management in small to medium-sized water utilities. Water Science and Technology 82, 2737–2744. doi:10.2166/wst.2020.377.

[11] Pudar, R.S., and Liggett, J.A. (1992). Leaks in pipe networks. Journal of Hydraulic Engineering 118, 1031–1046. doi:10.1061/(ASCE)0733-9429(1992)118:7(1031).

[12] Wu, Z.Y., Sage, P., and Turtle, D. (2010). Pressure-Dependent Leak Detection Model and Its Application to a District Water System. Journal of Water Resources Planning and Management 136, 116–128. doi:10.1061/(ASCE)0733-9496(2010)136:1(116).

[13] Sophocleous, S., Savić, D., and Kapelan, Z. (2019). Leak Localization in a Real Water Distribution Network Based on Search-Space Reduction. Journal of Water Resources Planning and Management 145, 04019024. doi:10.1061/(ASCE)WR.1943-5452.0001079.

[14] Casillas Ponce, M. V., Garza Castañón, L.E., and Cayuela, V.P. (2014). Model-based leak detection and location in water distribution networks considering an extended-horizon analysis of pressure sensitivities. Journal of Hydroinformatics 16, 649–670. doi:10.2166/hydro.2013.019.

[15] Geng, Z., Hu, X., Han, Y., and Zhong, Y. (2019). A Novel Leakage-Detection Method Based on Sensitivity Matrix of Pipe Flow: Case Study of Water Distribution Systems. Journal of Water Resources Planning and Management 145, 04018094. doi:10.1061/(ASCE)WR.1943-5452.0001025.

[16] Goulet, J.-A., Coutu, S., and Smith, I.F.C. (2013). Model falsification diagnosis and sensor placement for leak detection in pressurized pipe networks. Advanced Engineering Informatics 27, 261–269. doi:10.1016/j.aei.2013.01.001.

[17] Moser, G., Paal, S.G., and Smith, I.F.C. (2018). Leak Detection of Water Supply Networks Using Error-Domain Model Falsification. Journal of Computing in Civil Engineering 32, 04017077. doi:10.1061/(ASCE)CP.1943-5487.0000729.

[18] Capelo, M., Brentan, B., Monteiro, L., and Covas, D. (2021). Near–Real Time Burst Location and Sizing in Water Distribution Systems Using Artificial Neural Networks. Water 13, 1841. doi:10.3390/w13131841.

[19] Zhang, Q., Wu, Z.Y., Zhao, M., Qi, J., Huang, Y., and Zhao, H. (2016). Leakage Zone Identification in Large-Scale Water Distribution Systems Using Multiclass Support Vector Machines. Journal of Water Resources Planning and Management 142, 04016042. doi:10.1061/(ASCE)WR.1943-5452.0000661.

[20] Perez, R., Sanz, G., Puig, V., Quevedo, J., Cuguero Escofet, M.A., Nejjari, F., Meseguer, J., Cembrano, G., Mirats Tur, J.M., Sarrate, R., et al. (2014). Leak localization in water networks: A model-based methodology using pressure sensors applied to a real network in barcelona [applications of control]. IEEE Control Systems 34, 24–36. doi:10.1109/MCS.2014.2320336.

[21] Goldberg, D. (1989). Genetic Algorithms in Search, Optimization, and Machine Learning (New York, New York, USA: Addison Wesley).

[22] Rossman, L. (2000). EPANET 2 user's manual (United States Environmental Protection Agency).

[23] Klise, K.A., Bynum, M., Moriarty, D., and Murray, R. (2017). A software framework for assessing the resilience of drinking water systems to disasters with an example earthquake case study. Environmental Modelling & Software 95, 420–431. doi:10.1016/j.envsoft.2017.06.022.

[24] Blank, J., and Deb, K. (2020). Pymoo: Multi-Objective Optimization in Python. IEEE Access 8, 89497–89509. doi:10.1109/ACCESS.2020.2990567.

[25] Ferreira, B., Carriço, N., and Covas, D. (2021). Optimal Number of Pressure Sensors for Real-Time Monitoring of Distribution Networks by Using the Hypervolume Indicator. Water 13, 2235. doi:10.3390/w13162235.

[26] Ferreira, B., Antunes, A., Carriço, N., and Covas, D. (2022). Multi-objective optimization of pressure sensor location for burst detection and network calibration. Computers & Chemical Engineering 162, 107826. doi:10.1016/j.compchemeng.2022.107826.